KSCE Journal of Civil Engineering
DOI 10.1007/s12205-023-0941-z

pISSN 1226-7988, eISSN 1976-3808
www.springer.com/12205

Hydraulic Engineering

Velocity Distribution Upstream of Circular and Square Intakes

Nevzat Yıldırım[a] **and Kerem Taştan**[b]

[a]*Dept. of Civil Engineering, Faculty of Engineering, Çankaya University, Merkez Kampüs, Etimesgut/Ankara 06790, Türkiye*
[b]*Dept. of Civil Engineering, Faculty of Engineering, Gazi University, Maltepe/Ankara 06570, Türkiye*

ARTICLE HISTORY

Received 9 May 2023
Revised 11 August 2023
Accepted 31 August 2023
Published Online 9 November 2023

KEYWORDS

Boundary-blockage
Intake
Point sink
Potential flow
Velocity

ABSTRACT

In the present study, a practical method is developed to predict the radial velocity of the flow towards circular and square intakes. It is shown that one single spherical sink surface passing from the desired points that have radial velocity vectors of identical magnitude within the ambient fluid can be used for the prediction of the radial velocity. The specific imaginary center of the corresponding spherical sink surface should be located on the center-line axis downstream of the entrance of the intake. As opposed to the previous studies, the proposed method does not require the solution of equations in closed-integral form, and it can also be used for the orifice-intake not opening into the atmosphere (submerged outlet), and an intake with a pipe, or intake-pipe projecting into the ambient fluid. It is shown that velocity field can be predicted with the introduced method even in the case of circulation imposed or induced ambient fluid flow. The agreement between the theoretical results and the available experimental/numerical results was found to be good.

1. Introduction

In practice, intakes are very commonly used in dams, lakes, ponds, pools, oceans, reservoir-tanks, canals, streams, rivers, pump-sumps, water-conveying structures, gas ventilation systems, sediment-flushing structures, and fish-passages (Taştan, 2016; Acherar et al., 2022; Circiumaru et al., 2022; Sinha, 2022; Kumar et al., 2023; Roshan and Ghobadian, 2023; Xu et al., 2023a; Xu et al., 2023b). To predict the hydraulic behavior of an intake, it is necessary to have information about the velocity of the flow towards the intake. The studies related to the radial velocity distribution of the flow upstream of an orifice opening into the atmosphere include those by Recusani et al. (1991), Chanson et al. (2002), and Giesler and Stauch (1992). The numerical solutions for the velocity upstream of an orifice are also available in the studies by Islam and Zhu (2011), and Powel and Khan (2015). Considerable improvement in the radial velocity towards an orifice intake opening into the atmosphere was achieved in the studies by Shammaa et al. (2005), and Bryant et al. (2008). In their potential flow-based numerical solutions, the radial velocity distributions for both the circular and rectangular orifices opening into the atmosphere were approximated by considering that the flows towards these orifices consist of an infinite number of differential point sinks distributed all over the entire intake entrance cross-section. The methods developed by Shammaa et al. (2005), and Bryant et al. (2008) are not valid for the orifice-intake not opening into the atmosphere (submerged outlet), and an intake with a pipe, or intake-pipe projecting into the ambient fluid. In addition, the local radial velocity was given in a closed-integral form requiring numerical evaluation that may be laborious in practice. Furthermore, in the case of circulation imposed or induced ambient fluid flow, their results cannot be used for the prediction of the radial velocity of the flow towards an orifice-intake. There are several case studies relating to the intakes of different flow and geometrical conditions such as velocity distribution at the coarse rack and screen of an intake (i.e., Müller et al., 2018; Bytcankova et al., 2021). Potential flow solution-based studies for an air-entraining vortex at an intake showed that if a circular intake is present within an ambient fluid, an infinite number of complete and incomplete imaginary "Spherical sink surfaces" (SSS) having the same discharge and the center as the intake develop (Yıldırım and Kocabaş, 1995; Yıldırım, 2004; Naderi et al., 2014; Sarkardeh et al., 2014; Taştan and Yıldırım, 2018; Taştan et al., 2023).

Shammaa et al. (2005, Fig. 2) plotted V_s/V (vertical axis) against x/D (horizontal axis) relating to their numerical solutions for

CORRESPONDENCE Kerem Taştan ktastan@gazi.edu.tr Dept. of Civil Engineering, Faculty of Engineering, Gazi University, Maltepe/Ankara 06570, Türkiye

ⓒ 2023 Korean Society of Civil Engineers

both one single point sink (SPS) (having the same center and discharge as the intake entrance), and infinite number of point sinks distributed across the entrance plane of the orifice. Fig. 2 in the study by Shammaa et al. (2005) indicates that one SPS based numerical solution predicts the velocity very well for the points at distances larger than 1.5*D* to the center of the intake entrance (*D* = internal diameter of the circular intake-entrance); however, it does not satisfactorily predict the velocity at distances less than 1.5*D* to the center of the intake entrance. This is basically attributed to the blockage (to be defined a little later) and friction effects of the flow boundaries since the flow towards the intake-entrance considerably deviates from being a perfect SPS with the same center as the intake. Consequently, choosing the center of the intake-entrance as the fixed center for an SPS causes the velocity vector to considerably deviate from being acceptably radial towards the center of the intake-entrance.

As stated earlier, the results in the available studies are not valid and cannot be used for the cases that are as follows. 1) An orifice-intake not opening into the atmosphere (submerged outlet); 2) an intake with a pipe or intake-pipe projecting into an ambient fluid; 3) an intake sited in a circulation imposed or induced ambient fluid flow. Furthermore, in the available studies, the local radial velocity is given in a closed-integral form requiring numerical evaluation that may be laborious in practice. Due to these reasons, there is a need to develop a method for the prediction of the radial velocity of the flow towards an orifice-intake. This is the main aim and focus of the present study.

In the present study, a practical method is developed to predict the radial velocity of the flow towards an intake. It is shown that one SPS passing from the desired points that have radial velocity vectors of identical magnitude within the ambient fluid can be used for the prediction of the radial velocity. The corresponding specific imaginary center of the SSS should be on the center-line axis downstream of the entrance of the intake. The method introduced in the present study predicts the radial velocity of the flow towards the intake very well in a simple manner. The agreement between the theoretical results and the available experimental and numerical results was found to be good. The present study focuses on providing a simple semi-empirical practical method considering the concept of SSS for the prediction of the radial velocity at circular, and square intakes.

The velocity distributions for both the circular and square intakes are separately considered herein.

2. Velocity Upstream of a Circular Intake

Hereafter, the "point sink" and the "Spherical Sink (SS)" are interchangeably used. Shammaa et al. (2005, Fig. 2) noted that their point sink based numerical solution predicts uniform velocity distribution across the semicircle surface (in reality, it is indicating an SSS) for the points at distances larger than 1.5*D* to the center of the intake entrance. However, their numerical solution (infinite number of point sinks distributed across the entrance plane of the orifice) does not satisfactorily predict the velocity

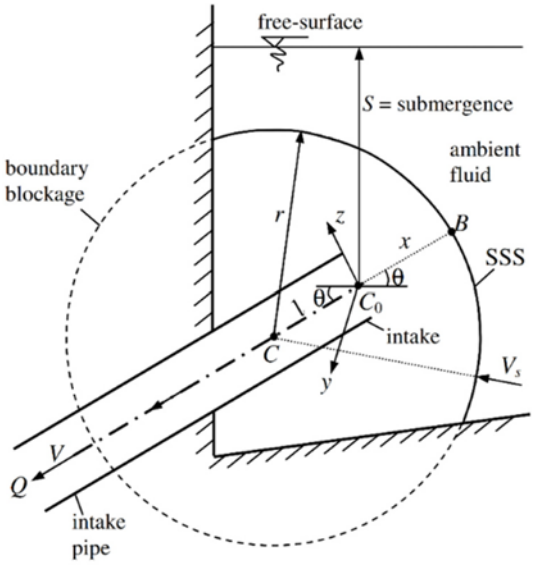


Fig. 1. Geometrical Variables and SSS

for the points at distances less than 1.5*D* to the center of the intake entrance (Rescusani et al., 1991; Giesler and Stauch, 1992 described the surfaces of equal velocities as hemispherical, however, Anayiotos et al. (1995) showed that iso-vel contours become hemi-elliptic as they approach the orifice).

Depending on the size of the intake entrance, the flow in this region considerably deviates from being a single SS having the same center as the intake entrance. In the flow region close to the intake entrance (distances < 1.5*D*), curvatures of the streamlines may rapidly vary, thereby the radial velocity vector at each location points to a center point of C on the central- axis line of the intake entrance (Fig. 1). This means that the geometrical locations of the radial velocity vectors of identical magnitude on different streamlines pointing the same center C should be an SSS as indicated in Fig. 1. Especially in the flow region close to the intake entrance, there corresponds a center point C for each SSS. In reality, instead of one single SS having the same center as the intake entrance, it is better to utilize different SSS(s) with their respective imaginary centers on the central-axis-line of the intake entrance for the prediction of the radial velocity.

Based on this fact, in the present study, it is considered that the geometrical locations of the points within the ambient potential flow field having an identical magnitude of the radial velocity vectors is an SSS. The corresponding imaginary center C of an SSS is on the central-axis line of the intake (normal to the entrance plane of the intake) as indicated in Fig. 1. This new approach leads to utilizing an SSS (with a shifted center) larger than the SSS (having the identical center as the intake) used in the available studies stated earlier. In Fig. 1; *x*, *y*, and *z* are the Cartesian coordinates; C_o is the center of intake entrance; *S* is the submergence of the center C_o of the intake entrance (or the vertical distance of the center C_o of the intake entrance to the free-surface); *r* is the radius of SSS; *l* is the distance between C_o and C; and *x* is the distance of the intersection point B of the SSS

and the central-axis line of the intake-entrance to C_o ($l = CC_o$; $x = C_oB$; $r = CC_oB$; Fig. 1 and Eq. (1)).

$$r = l + x \text{ ; or } r/D = l/D + x/D \tag{1}$$

If the distance of a boundary (including the pipe of the intake and the air-boundary or free-surface) to the center C of SSS is less than r; the boundary cuts the SSS and causes a loss in the surface area of SSS (incomplete SSS). This loss is called the "boundary blockage" (Yıldırım et al., 2000). If the distance of a boundary to the center C of the SSS is larger than or equal to r, the boundary does not intersect the SSS (complete SSS), and the boundary has no blockage effect on SSS. The blockage of a boundary is also related to the clearances of the boundaries to the center C_o of the intake entrance. The continuity equation for the flow passing through the SSS shown in Fig. 1 can be written as follows.

$$Q = Q_s = A_s V_s = VA \tag{2}$$

$$V_s/V = A/A_s \tag{3}$$

In which, Q is the intake discharge; Q_s is the discharge through the SSS; A is the intake cross-section area; V is the average intake velocity; A_s is the net effective area of the SSS; and V_s is the radial velocity at SSS. Continuity dictates that the magnitude of V_s/V on an SSS must be a constant, and whatever the conditions or positions of the circular intake are; the geometrical locations of the points that have identical V_s/V must be an SSS that has identical r or r/D. It may also be stated that for each magnitude of V_s/V there is a corresponding SSS or r/D.

Shammaa et al. (2005) compared the experimental measurements of resultant velocities along the x axis of a deep circular orifice with the solution of a single-point sink located at the center of the orifice. For a given magnitude of V_s/V, the horizontal difference between the curves for the point sink solution and the test data in Fig. 2 of Shammaa et al. (2005, Fig. 2) are equal to $l/D = (r/D - x/D)$ in the present study because, both SSS in the present study and the SPS in the study by Shammaa et al. (2005) have a common point on the central-line axis of the intake entrance. The magnitudes of l/D and V_s/V obtained from Fig. 2 in the study by Shammaa et al. (2005) are plotted in Fig. 2. Note that V_r, U_o, d, and x in the study by Shammaa et al. (2005) correspond to V_s, V, D and x in the present study, respectively.

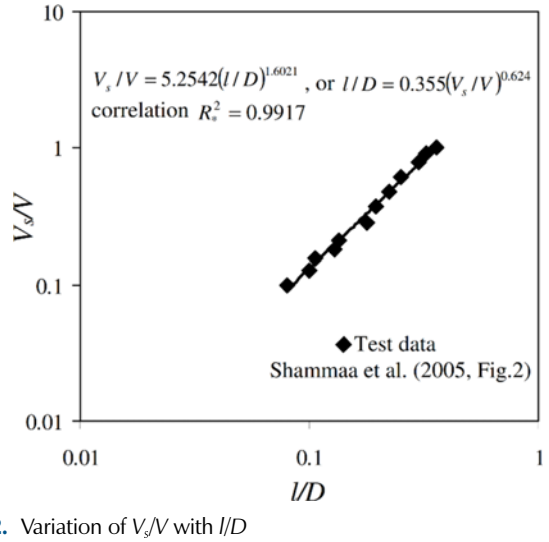


Fig. 2. Variation of V_s/V with l/D

The equation of the fitted line in Fig. 2 is as follows (correlation coefficient of the fitted line in Fig. 2 is $R_*^2 = 0.9917$);

$$\frac{V_s}{V} = 5.254\left(\frac{l}{D}\right)^{1.602}, \tag{4}$$

$$\frac{l}{D} = 0.355\left(\frac{V_s}{V}\right)^{0.624}. \tag{5}$$

The limitations relating to V_s/V and l/D are provided a little later.

From Eqs. (3) – (5)

$$\frac{l}{D} = 0.355\left(\frac{A}{A_s}\right)^{0.624} \quad (\text{if } Q_s < Q \text{ use } A_{sb} \text{ in lieu of } A). \tag{6}$$

Herein, A_{sb} is the area of the base of the sector of the SSS = πr_{sb}^2 (for the case of $Q_s < Q$), and r_{sb} is the radius of the base of the sector of SSS at the intake entrance (Fig. 3). Continuity dictates that there can be two cases as indicated in Figs. 1 and 3 that are as follows: 1) if $r_{sb} \geq D/2$ the discharge through the SSS is the same as the intake discharge ($Q = Q_s$; Fig. 3(a)), and 2) if $r_{sb} < D/2$ the discharge through the SSS is not the same as the intake discharge ($Q > Q_s$; Fig. 3(b)) because in such a case, the sector of SSS falls into (remains within) the internal circumference crest-boundaries of the intake entrance, and causes Q not to be solely equal to the discharge through the sector of the SSS. For this case, Q should be equal to the sum of the discharges entering both through the sector of SSS (Q_s) and through the gap between the internal circumference-crest-edges of the intake entrance and the base-boundary of the sector of SSS within the intake entrance (Fig. 3(b)).

To determine the limiting magnitudes of the parameters (in Eqs. (4) – (6)) corresponding to the case of $r_{sb} = D/2$, the SSS is denoted by SSS_{limit} as indicated in Fig. 3(a) (circumference of the base of the SSS_{limit} just intersects the internal circumference crest-edges of the intake-entrance).

Let $(x/D)_{limit}$, $(l/D)_{limit}$, $(r/D)_{limit}$, A_{slimit} and $(V_s/V)_{limit}$ denote x/D, l/D, r/D, A_s and V_s/V corresponding to the SSS_{limit}, accordingly. The magnitudes of $(x/D)_{limit}$, $(l/D)_{limit}$, $(r/D)_{limit}$ and $(V_s/V)_{limit}$ are important criteria to determine whether or not the intake works as a SPS with the same discharge as the intake. The magnitudes of the $(x/D)_{limit}$, $(l/D)_{limit}$, $(r/D)_{limit}$, A_{slimit}, and $(V_s/V)_{limit}$ are determined by using the following method.

Considering Fig. 3, from geometry [$r^2_{limit} = (l + x)^2_{limit} = l^2_{limit} + (D/2)^2$], it can be written as

$$\left(\frac{l}{D}\right)_{limit} = \frac{1}{8}\left(\frac{D}{x}\right)_{limit} - \frac{1}{2}\left(\frac{x}{D}\right)_{limit}. \tag{7}$$

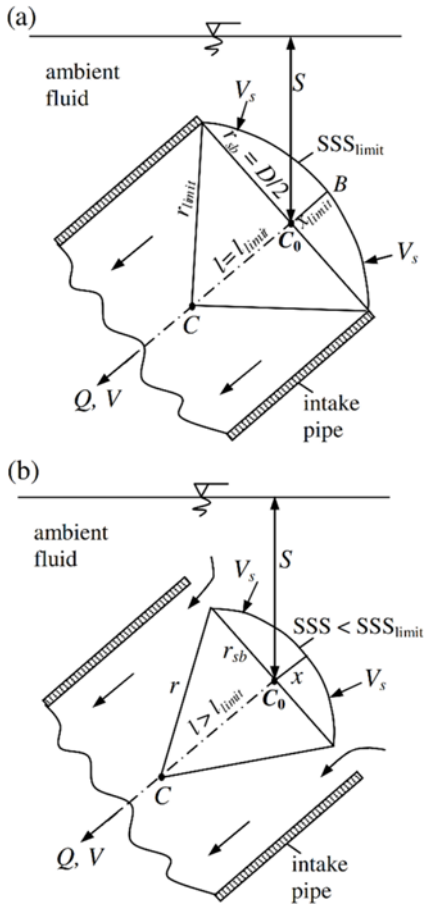


Fig. 3. SSS and SSS_{limit}: (a) $SSS = SSS_{limit}$, (b) $SSS < SSS_{limit}$ for a Circular Intake

$$A_{slimit} = 2\pi r_{limit}\, x_{limit}$$

(from geometry, the lateral surface areaof the spherical sector), (8)

$$Q = A_{slimit}\left(V_s\right)_{limit} = VA = V\pi D^2/4\,, \tag{9}$$

$$\left(\frac{V_s}{V}\right)_{limit} = \frac{1}{8\left[\left(\frac{l}{D}\right)_{limit} + \left(\frac{x}{D}\right)_{limit}\right]\left(\frac{x}{D}\right)_{limit}}\,. \tag{10}$$

From Eqs. (7) and (9),

$$\left(\frac{x}{D}\right)_{limit} = \frac{\sqrt{\left(\frac{V}{V_s}\right)_{limit} - 1}}{2}\,, \tag{11}$$

$$\left(\frac{l}{D}\right)_{limit} = \frac{2 - \left(\frac{V}{V_s}\right)_{limit}}{4\sqrt{\left(\frac{V}{V_s}\right)_{limit} - 1}}\,. \tag{12}$$

For the SSS_{limit}, equating Eqs. (4) or (6) and (7), and by using a trial and error solution procedure, Eq. (9) yields $(V_s/V)_{limit} = 0.755 \approx 0.75$ (taken). Thus, for the SSS_{limit}, from Eqs. (1) – (12), the followings are obtained.

$$\left(\frac{x}{D}\right)_{limit} \approx 0.285\,;\ \left(\frac{l}{D}\right)_{limit} \approx 0.296\,;\ \left(\frac{r}{D}\right)_{limit} \approx 0.581\,;$$

$$\left(\frac{A}{A_s}\right)_{limit} \approx 0.75\,;\ \left(\frac{V_s}{V}\right)_{limit} \approx 0.75 \tag{13}$$

Therefore, it can be written as

$$x/D \geq 0.285;\ l/D \leq 0.296;\ r/D \geq 0.581;\ V_s/V \leq 0.75;\ \text{and } A/A_s \leq 0.75 \text{ (for } Q = Q_s). \tag{14}$$

Equations (1) – (6) can be solved for l/D, r/D, x/D, and thereby SSS for a given magnitude of V_s/V by a trial-and-error solution procedure that is as follows.

1. With identical scale in all directions, manually or by a computer-aided graphical method, draw the geometry of intake and the ambient flow field (including the intake-pipe and the flow boundaries) within the same figure. Mark the center C_o of the intake entrance cross-section as in Fig. 1.
2. Since V_s/V is known (given), then compute l or l/D from Eqs. (4) – (6). Mark the location of the centers C of the SSS on the axis line passing from the center point C_o of the intake-entrance ($l = CC_o$).
3. Choose a magnitude for r or r/D and draw the SSS on the figure drawn in step (1).
4. Through a geometrical method or manual-graphical method or computer-aided graphical method, evaluate the net effective A_s of the SSS.
5. Since Q and A are known, then compute $V = Q/A$, $V_s = Q/A_s$ and V_s/V.
6. Compare the magnitudes of the computed V_s/V and the given V_s/V (used at the beginning of the solution).
7. If the magnitudes of the computed V_s/V and the given V_s/V are acceptably close, then the solution is correct. If not, choose a new magnitude for r or r/D and repeat the solution starting from step (3).

Once the solution is found, check the magnitudes of the parameters with their limits given Eqs. (7) – (14).

2.1 Analysis for the Case of $SSS < SSS_{limit}$ ($Q > Q_s$ or $r_{sb} < D/2$)

In the case of $SSS < SSS_{limit}$, it is reasonable to consider and assume that the base of the SSS is an imaginary circular intake entrance ($Q_s = VA_{sb}$) for which Eqs. (2) – (6) are valid because in obtaining them, the test data for $V_s/V > 0.75$ are also used as indicated in Fig. 2 [provided that A_{sb} is used instead of A in Eq. (6) for $SSS < SSS_{limit}$ or $Q > Q_s$ or $r_{sb} < D/2$]. From continuity,

$$Q_s = VA_{sb} = V_s A_s \ \text{ from which } \ V_s/V = A_{sb}/A_s\,. \tag{15}$$

Note that the boundaries (including the intake pipe itself, screen or rack-type structures at the intake entrance plane) may

have blockage effects where both A_s and A_{sb} has to be evaluated as a net effective area. If there are no screen or rack-type structures at the intake entrance plane, then from geometry in Fig. 3(b), it can be written as

$$A_s = 2\pi rx = 2\pi r(r-l)\;;\; A_{sb} = \pi r_{sb}^2\;;\; r_{sb}^2 = \left(r^2 - l^2\right);$$

$$\frac{V_s}{V} = \frac{A_{sb}}{A_s} = \frac{\left(\frac{r}{D} + \frac{l}{D}\right)}{2\frac{r}{D}}. \tag{16}$$

By considering Eqs. (4), (6), (15), and (16) for a required V_s/V (for the range of $0.75 < V_s/V \leq 1$), one can obtain r/D (also l/D and x/D) and draw the SSS for that V_s/V.

For example, for $V_s/V = 0.90$, Eqs. (4), (5) and (16) give $l/D = 0.332$, $r/D = 0.416$, $x/D = 0.084$, and $r_{sb}/D = 0.25$, for which the SSS drawn with the center of $C_{0.9}$ as indicated in Fig. 4(c).

2.2 Comparison of Experimental and Theoretical Results ($Q = Q_s$, $r_{sb} \geq D/2$ or SSS $\geq$ SSS$_{limit}$)

To examine the validity of the method presented in this study, the available test data provided by Anayiotos et al. (1995) (for a circular orifice intake freely discharging into the atmosphere) given in Fig. 3 in the study by Shammaa et al. (2005), the numerical solution results given in Fig. 3 in the study by Bryant et al. (2008) (so-called the "new solution" for the orifice intake discharging into the atmosphere), the numerical solution given in Fig. 4 in the study by Shammaa et al. (2005), and the available test data for a considerably high circulation imposed flow towards a circular-orifice intake in Fig. 8 of the study by Daggett and Keulegan (1974) are compared with the results of Eqs. (1) – (6) in Figs. 4, 5, and 6 (given a little later).

The magnitudes of l/D to locate the center(s) C are found through Eq. (5) for the corresponding magnitudes of V_s/V in Figs. 4(a) – 4(c).

As an example, let us find the geometrical location (SSS) of the points that have $V_s/V = 0.3$ given in the study by Shammaa et al. (2005, Fig. 3) or Anayiotos et al. (1995, Fig. 1). In their experiments, $D = 3 – 10$ mm and canal width of 25 cm were used. The entrance of the circular orifice intake installed on the center line was almost flush with the vertical rear-wall through which the orifice issues, hence the clearance of the intake entrance center C_0 to the vertical rear-wall was negligible, and the distance of the vertical rear-wall to the center C of SSS was equal to l that is less than r. Therefore, the vertical rear-wall intersected the SSS and it had a blockage effect on SSS. The distances of the left and right-side walls, and the bottom floor boundary to the center C of the SSS were sufficiently large {larger than or equal to the magnitudes of r or thereby $(r^2 – l^2)^{1/2}$ or $[(r/D)^2 – (l/D)^2]^{1/2}$ for their test data} since these boundaries did not intersect the SSS. Thus, the left and right-side walls, and the bottom floor boundary had no blockage effects on SSS. From Eqs. (2) and (5) get $l/D = 0.355(0.3)^{0.624} = 0.167$, and $A/A_s = V_s/V = 0.3$; compute $A_s = 3.333A$ or, $(A_s/D^2) = 3.333A/D^2 = 3.333(\pi D^2)/(4D^2) = 2.616$. Since $l/D = 0.167$ is known, the center C of the SSS is located and denoted by $C_{0.3}$ in Fig. 4(a). Since it requires a trial-and-error solution procedure, to prevent this paper from being excessively long, only the solution of the final trial is given herein. Let us choose $r/D = 0.734$ for which SSS is drawn in Fig. 4(a). Check $[(r/D)^2 – (l/D)^2]^{1/2} = [(0.734)^2 – (0.167)^2]^{1/2} = 0.714$ that is smaller than the distances of the side walls and the bottom floor boundary to the center $C_{0.3}$ of the SSS. Therefore, the side walls and the bottom floor boundary have no blockage effects on SSS. Only the vertical rear-wall has a blockage effect on SSS as stated earlier. In this example, it is geometrically simple to compute A_s that is $A_s = 2\pi rx = 2\pi r(r – l)$ or $(A_s/D^2) = 2.616 = 2\pi(r/D)(r/D – l/D) = 2\pi(r/D)(r/D – 0.167)$ that yields $r/D = 0.734$. Since both magnitudes of the chosen and computed r/D (= 0.734) are equal, the solution is correct (no need to choose a new magnitude for r/D and repeat the solution). Note that $x/D = (r/D – l/D) = (0.734 – 0.167) = 0.567$.

Similarly, for the geometrical location (SSS) of the points that have $V_s/V = 0.2$ in the study by Shammaa et al. (2005, Fig. 3), the parameters are found to be $l/D = 0.355(0.2)^{0.624} = 0.130$, and A/A_s

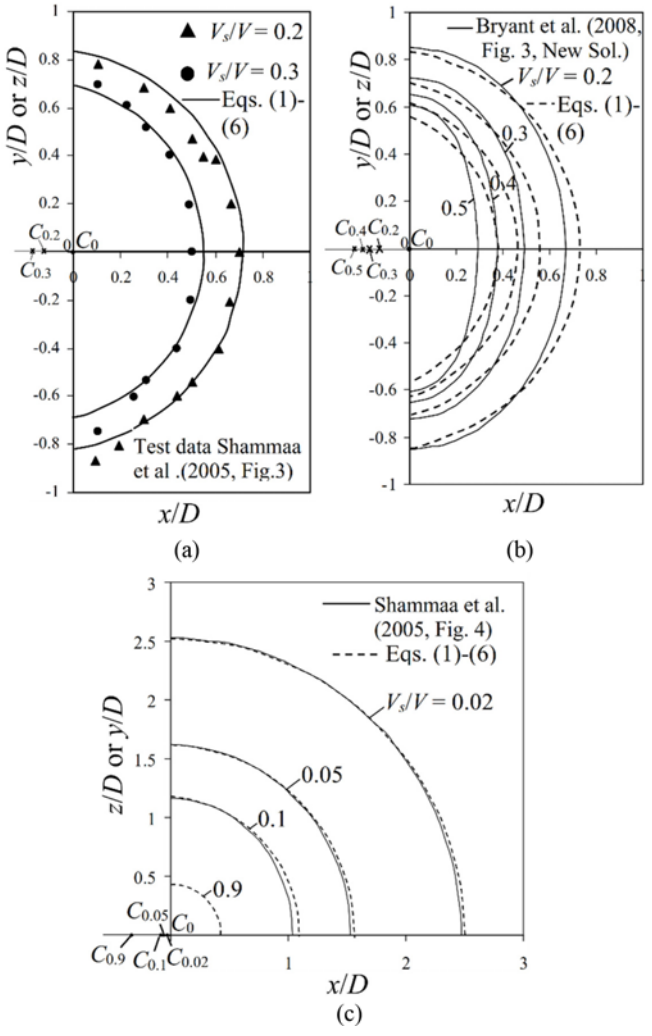


Fig. 4. Comparison of the Present Study: (a) With Available Test Data, (b), and (c) With Available Numerical Solutions

= V_s/V = 0.2; compute A_s = 5A or (A_s/D^2) = 3.925; r/D = 0.858; and x/D = (0.858 – 0.130) = 0.728. The center of SSS for V_s/V = 0.2 is denoted by $C_{0.2}$, and the SSS is drawn as indicated in Fig. 4(a). Note that the magnitude of l/D, x/D, r/D, and V_s/V are found above to satisfy their respective limits given in Eqs. (7) – (14).

By following the same computation procedure as presented above, considering V_s/V = 0.2, 0.3, 0.4, and 0.5 for the potential solution-based numerical results in the study by Bryant et al. (2008, Fig. 3, circular orifice intake was flush with the vertical rear wall through which the orifice opens into the atmosphere), the parameters l/D = 0.130, 0.167, 0.200, and 0.230; r/D = 0.858, 0.734, 0.668 and 0.628; and x/D = 0.728, 0.567, 0.468, and 0.398 are found, respectively. The results of the present study (SSSs) and the numerical results in the study by Bryant et al. (2008, Fig. 3) are compared in Fig. 4(b). Note that the vertical and horizontal scales in Fig. 3 in the study by Bryant et al. (2008) are different. Since the drawing of SSS requires identical scales in all directions, Fig. 3 in their study is redrawn in Fig. 4(b) by using an identical scale in both horizontal and vertical axes. The centers of SSSs for V_s/V = 0.2, 0.3, 0.4, and 0.5 are denoted by $C_{0.2}$, $C_{0.3}$, $C_{0.4}$, and $C_{0.5}$, respectively in Fig. 4(b). This figure indicates that the method introduced in the present study predicts the radial velocity acceptably well within the ambient fluid flow field The above analysis and Fig. 4(b) infer that as r increases, l decreases. Furthermore, for $x/D \geq 1.5$; l/D is less than 0.05 (that is negligible and $r/D \cong x/D$ may be taken) indicating that the center of the intake entrance can be taken as the center of whole SSS(s) or co-centric iso-vels for $r/D \geq 1.5$ (C coincides with C_o, one SPS or SSS that has the same center and discharge as the intake approximation becomes valid).

The results of the present study and the potential flow-based numerical solution results in the study by Shammaa et al. (2005, Fig. 4) are compared in Fig. 4(c). In their study, the circular orifice intake was flush with the vertical rear wall through which the orifice opened into the atmosphere. Considering V_s/V = 0.02, 0.05, and 0.1 in the study by Shammaa et al. (2005, Fig. 4), l/D = 0.0309, 0.0547, and 0.0844; r/D = 2.515, 1.609, and 1.163; and x/D = 2.485, 1.554, and 1.078 are found, respectively. The centers of SSSs relating to V_s/V = 0.02, 0.05, and 0.1 are denoted by $C_{0.02}$, $C_{0.05}$, and $C_{0.1}$, respectively in Fig. 4(c). As it can be seen from Fig. 4(c), the agreement between the proposed method and the Shammaa et al. (2005, Fig. 4) is very good.

The comparison of the proposed theory in this study with the test data in the study by Daggett and Keulegan (1974, Fig. 8, Q = 0.019 m^3/s, D = 0.1016 m, S = 0.3048 m) is challenging because they imposed very large circulation on the flow towards a circular orifice intake located in a large cylindrical tank that should be one of the severe and adverse cases in practice. The vertical depths (across which radial velocities were measured) at horizontal distances of R from the vertical axis of the circular orifice-intake are indicated in Fig. 5 [$R/(D/2)$ = 2.64 (or R/D = 1.32, R = 13.4 cm); $R/(D/2)$ = 3.54 (or R/D = 1.77, R = 17.98 cm); $R/(D/2)$ = 4.44 (or R/D = 2.22, R = 22.55 cm); $R/(D/2)$ = 5.34 (or R/D = 2.67, R = 27.12 cm); and $R/(D/2)$ = 6.24 (or R/D = 3.12, R = 31.7 cm)].

If the method introduced in the present study is correct and valid, then all the intersection points of the SSS and the vertical depths corresponding to the horizontal radial distances stated

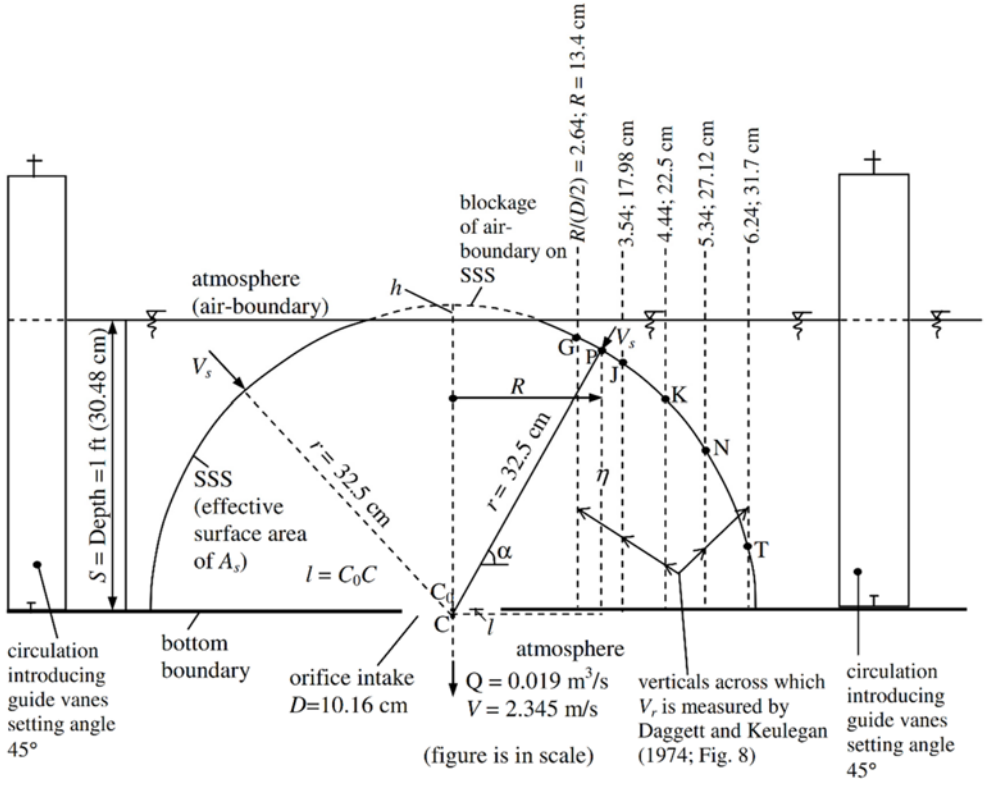


Fig. 5. Test Set-Up in Fig. 8 of the Study by Daggett and Keulegan (1974), and the SSS

earlier should have identical measured or computed V_s or V_s/V. The trial-and-error solution procedure for this purpose is as follows (note that to prevent this paper from being excessively long, only the solution of the final trial is given herein).

For example, let us examine the geometrical location (SSS or r) of the points that have $V_s/V = 0.013$ for which Eq. (5) gives $l/D = 23.6 \times 10^{-3}$ or $l = 23.6 \times 10^{-3} \times 0.1016 = 239.77 \times 10^{-5}$ m (centers C and C_o almost coincide). Choose $r = 32.5$ cm for which the SSS drawn in Fig. 5 passes from whole verticals across which Daggett and Keulegan (1974, Fig. 8) measured V_s (Taştan and Yıldırım, 2018).

In Fig. 5, consider a point P on SSS. The vertical distance of the point P to the bottom boundary, and the horizontal distance of the point P to the vertical axis of the orifice-intake are denoted by η and R, respectively. The slope angle of the radial line connecting P and C, and the altitude of the spherical sector (cap) of the SSS remaining above the fluid surface (due to the blockage of the air-boundary on SSS) are denoted by α and h, accordingly (Fig. 5). In Fig. 5, the intersection points of SSS with the vertical depths (across which V_s were measured) at the horizontal distances of $R/(D/2) = 2.64$; 3.54; 4.44; 5.34; and 6.24 are indicated as G, J, K, N, and T, respectively. As it is seen in Fig. 5, since the clearances of all side boundaries are larger than or equal to $r = 32.5$ cm, they have no blockage effects on the SSS. Only the bottom boundary, and the air-boundary or free-surface [since $(r - l) = (0.325 - 239.77 \times 10^{-5}) = 0.322$ m is larger than the total flow depth or submergence of 0.3048 m above the orifice-intake] have blockage effects on the SSS. In this example, the net effective surface area of the SSS, A_s, is simple and easily evaluated from geometry (no need to evaluate A_s from the scaled-drawing graphic or computer aided-graphic). From geometry in Fig. 5 (if $h \le 0$ then set $h = 0$);

$$A_s = 2\pi r(r - l) - 2\pi r h = 2\pi r^2 - 2\pi r(l + h);$$
$$r^2 = R^2 + (\eta + l)^2;\ h = [(r - l) - S]. \tag{17}$$

Equation (17) gives

$$r = \frac{R^2 + (\eta + l)^2 - A_s/(2\pi)}{(l + h)}. \tag{18}$$

$A = \pi D^2/4 = \pi(0.1016)^2/4 = 0.0081$ m^2, $V = Q/A = 0.019/0.0081 = 2.345$ m/s, then $V_s = 0.0304$ m/s. From Eq. (6), $A_s = A/(V_s/V) = 0.0081/0.013 = 0.623$ m^2; and $A_s/(2\pi) = 0.0992$ m^2. From Eq. (17); $h = (0.325 - 239.77 \times 10^{-5} - 0.3048) = 178.02 \times 10^{-4}$ m.

For example; let us find V_s at the intersection point G of SSS and the vertical depth at a horizontal distance of $R/(D/2) = 2.64$ (or $R/D = 1.32$, or $R = 13.41$ cm) in Fig. 5. For the point G in Fig. 5, $\eta = 29.4$ cm [or $\cos\alpha = R/r = 0.1341/0.325 = 0.41265$, thus $\alpha = 65.628^o$, $\eta = (r\sin\alpha - l) = 0.325 \sin 65.628^o - 239.77 \times 10^{-5} = 0.294$ m] and $R = 0.1341$ m are read. With $\eta = 0.294$ m and $R/(D/2) = 2.64$, if one goes to Fig. 8 in the study by Daggett and Keulegan (1974) the measured $V_s = 0.029$ m/s is read. To control the solution, let us check the magnitudes of r, η, and V_s.

Equation (18) gives $r = [(0.1341)^2 + (0.294 + 239.77 \times 10^{-5})^2 - 99.22 \times 10^{-3}] / (239.77 \times 10^{-5} + 178.02 \times 10^{-4})] = 0.327$ m $\approx$ 0.325 m (chosen at the beginning of the solution) (acceptable); $\cos\alpha = R/r = 0.1341/0.325 = 0.412654$; or $\alpha = 65^o.628$; $\eta = (r\sin\alpha - l) = (0.325 \times \sin 65^o.628 - 239.77 \times 10^{-5}) = 0.298$ m (computed) ≈ 0.294 m (measured); and $V_s = 0.0304$ m/s (computed) ≈ 0.029 m/s (measured). Therefore, further trial is not needed. The difference between the computed and the measured magnitudes of V_s is about 4% which is acceptable and can be attributed to the reasons that are as follows.

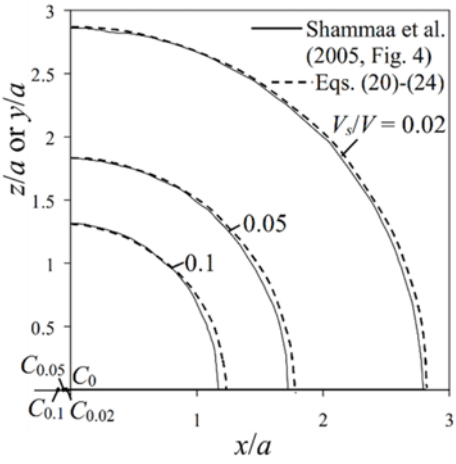


Fig. 6. Comparison of the Present Study with the Available Numerical Results for a Square Intake

1. In their tests, Daggett and Keulegan (1974) measured V_s by means of a miniature propeller flow meter of 10 mm in diameter that may cause some local disturbance-effect, and thereby some error in measuring V_s may be present.
2. Some error may be related to the sensitivity of the propeller flow meter.
3. The circular intake is considered to be of a perfect SS that may deviate from reality due to the effects of the size of the intake, viscosity and surface tension.
4. The relationship between l/D and V_s/V in Eq. (3) is found by fitting a line to the test data that may also involve some error.
5. Some error may be present in readings relating to the magnitudes of V_s from the data-plot graphs in the study by Daggett and Keulegan (1974).

If the method introduced in the present study is true then the points of J, K, N and T on the same SSS of $r = 32.5$ cm and the center of C in Fig. 5 should have the same $V_s = 0.0304$ m/s (≈ 0.0293 m/s) as the point G on the same SSS. This is achieved as following.

Figure 5 indicates that the points J, K, N, and T have $\eta = 27$ cm, 23 cm, 17.5 cm, and 6.5 cm for which Daggett and Keulegan (1974) measured the magnitudes of the $V_s = 0.032$ m/s; 0.030 m/s; 0.032 m/s; and 0.033 m/s, respectively (the maximum difference is about 9% that may be attributed to the reasons stated earlier). All these infer that all points G, J, K, N, and T on the same SSS (of $r = 32.5$ cm and center of C in Fig. 5) have approximately the

same $V_s \approx 0.030$ m/s or $V_s/V = 0.03/2.345 = 0.01295 \approx 0.013$ as computed earlier.

The above comparisons confirm that the method developed in the present study can be used for the prediction of the radial velocity V_s for the flow at a circular intake.

3. Velocity Upstream of a Square Intake

Consider a square intake that has a side dimension of a. Experimental and potential flow solution results in the study by Yıldırım (2004) indicated that flow at a square intake may be approximated as a SSS. Thereby, the same computation procedure and principle as the circular intake explained earlier may also be used for a square intake.

To adapt Eqs. (4) – (6) for a square intake, it is reasonable to approximate the square intake as an equivalent circular intake of same cross-section area. That is $A = a^2 = \pi D^2/4$ or $D = 2a/\sqrt{\pi} = 1.129a$. Hence, Eqs. (4) – (6) for a square intake may be written as

$$\frac{V_s}{V} = 4.326\left(\frac{l}{a}\right)^{1.602}\ ;\ \frac{l}{a} = 0.4\left(\frac{V_s}{V}\right)^{0.624} = 0.4\left(\frac{A}{A_s}\right)^{0.624}.$$

(if $Q_s < Q$ use net A_{sb} in lieu of A) (19)

Note that in the case of a square intake, as indicated in Fig. 7 provided in the Appendix, SSS_{limit} has to pass from the corners of the square intake (radial distance of each corner point to the center C_o of the intake entrance is equal to $a/\sqrt{2}$). In the cases of SSS(s) smaller than SSS_{limit}, the sector(s) of SSS falls into the intake entrance and causes Q not solely to be equal to the discharge through the sector of the SSS (Q is going to be equal to the sum of the discharges entering both through the sector of SSS and through the gap between the internal boundary of the intake entrance and the sector of SSS similar to Fig. 3).

To determine the limiting magnitudes of the parameters (in Eq. (19)) corresponding to the case of $r_{sb} = a/\sqrt{2}$ (the circumference of the base of the SSS_{limit} just intersects the internal circumference crest-edges of the square intake-entrance as indicated in Fig. 7 provided in the Appendix, the following method is used.

From geometry (Fig. 7 in Appendix) it may be written as

$$r = (l + x)\ ;\ r_{limit}^2 = (l + x)_{limit}^2 = l_{limit}^2 + \left(a/\sqrt{2}\right)^2\ ;$$

$$r/a = (l/a + x/a). \quad (20)$$

The limiting magnitudes of the variables for a square intake can be found as follows.

$$\left(\frac{l}{a}\right)_{limit} = \frac{1}{4}\left(\frac{a}{x}\right)_{limit} - \frac{1}{2}\left(\frac{x}{a}\right)_{limit} \quad (21)$$

$$\text{Continuity}\ \ Q = A_{slimit}\left(V_s\right)_{limit} = VA = Va^2, \quad (22)$$

$$\left(\frac{V_s}{V}\right)_{limit} = \left(\frac{a^2}{A_{slimit}}\right), \quad (23)$$

$$A_{slimit} = 2\pi r_{limit} x_{limit}$$

(from geometry, the lateral surface area of the spherical sector) (24)

$$\left(\frac{V_s}{V}\right)_{limit} = \frac{1}{2\pi\left[\left(\frac{l}{a}\right)_{limit} + \left(\frac{x}{a}\right)_{limit}\right]\left(\frac{x}{a}\right)_{limit}}. \quad (25)$$

From Eqs. (24) and (25),

$$\left(\frac{x}{a}\right)_{limit} = \sqrt{\frac{1}{\pi}\left(\frac{V}{V_s}\right)_{limit} - \frac{1}{2}}, \quad (26)$$

$$\left(\frac{l}{a}\right)_{limit} = \frac{1 - \frac{1}{\pi}\left(\frac{V}{V_s}\right)_{limit}}{2\sqrt{\frac{1}{\pi}\left(\frac{V}{V_s}\right)_{limit} - \frac{1}{2}}}. \quad (27)$$

For the SSS_{limit}, equating l/a in Eqs. (19) and (26), and by using a trial and error solution procedure, it yields a $(V_s/V)_{limit} = 0.42$. Thus, for the SSS_{limit}, from Eqs. (19) – (27), the followings are obtained.

$$\left(\frac{x}{a}\right)_{limit} \approx 0.508\ ;\ \left(\frac{l}{a}\right)_{limit} \approx 0.232\ ;\ \left(\frac{r}{a}\right)_{limit} \approx 0.74\ ;$$

$$\left(\frac{A}{A_s}\right)_{limit} \approx 0.42\ ;\ \left(\frac{V_s}{V}\right)_{limit} \approx 0.42 \quad (28)$$

Hence it can be written as

$$x/a \geq 0.508;\ l/a \leq 0.232;\ r/a \geq 0.74;\ V_s/V \leq 0.42;$$
$$\text{and}\ A/A_s \leq 0.42\ (\text{for}\ Q_s = Q). \quad (29)$$

To examine the validity of the method presented in this study (by following the similar procedure for a circular intake explained earlier), the results given in Fig. 4 in the study by Shammaa et al. (2005) for a square orifice intake freely discharging into the atmosphere are compared in Fig. 6.

Note that in the study by Shammaa et al. (2005, Fig. 4), the entrance of the square orifice intake was flush with a vertical rear-wall boundary through which the square orifice intake was issued. The clearance of the intake entrance center C_0 to the vertical rear wall was zero. Therefore, the vertical rear-wall had a blockage effect on SSS. The clearances of the side walls and the bottom floor boundaries to the intake entrance were sufficiently large (larger than or equal to r) because the side walls and the bottom floor boundary had no blockage effect on SSS.

The solution for $V_s/V = 0.1$ is provided in Appendix, and by following the same computation procedure, considering $V_s/V = 0.05$, and 0.02 the parameters $l/a = 0.0617$, and 0.0348; $r/a = 1.815$, and 2.839; and $x/a = 1.753$, and 2.804 are found, respectively. The centers of SSSs for $V_s/V = 0.05$ and 0.02 are denoted by $C_{0.05}$ and $C_{0.02}$, respectively, and their corresponding

SSSs are drawn as indicated in Fig. 6. The results of the present study (SSSs) and the results in the study by Shammaa et al. (2005, Fig. 4) are compared in Fig. 6.

Note that the magnitudes of l/a, x/a, r/a, and V_s/V found above satisfy their respective limits given in Eq. (29). Fig. 6 indicates that the practical method introduced in the present study predicts the radial velocity towards a square intake acceptably well within the ambient fluid flow field.

3.1 Analysis for the Case of SSS < SSS_{limit} ($Q > Q_s$ or $V_s/V > 0.42$ or $r_{sb} < a/\sqrt{2}$)

In the case of SSS < SSS_{limit}, it is reasonable to consider and assume that the base of the SSS is an imaginary circular intake entrance ($Q_s = VA_{sb}$) for which Eq. (19) is valid [provided that A_{sb} is used in lieu of A in Eq. (19) for SSS < SSS_{limit} or $Q > Q_s$ or $V_s/V > 0.42$ or $r_{sb} < a/\sqrt{2}$]. Note that for the range of $a/2 < r_{sb} < a/\sqrt{2}$, the boundaries (including the intake-duct pipe itself) may have blockage effects since both A_s and A_{sb} have to be evaluated as a net effective area. For $r_{sb} \leq a/2$, the magnitude of A_{sb} is similar to that given in Eq. (16) if there are no screen or rack-type structures at the intake entrance plane. The computation procedure is similar to that for a circular intake given earlier.

Comparisons related to the results of the proposed equations for circular and square intakes with the available experimental/numerical results are summarized in Table 1. In this table; MAE is the Mean Average Error, MSE is the Mean Square Error, RMSE is the Root Mean Square Error, and MPE is the Mean Percentage Error. Since some of the velocity contours in horizontal or vertical planes in Figs. 4 – 6 are close to a circle, coefficient of determination values did not give meaningful results, therefore, they were not used in Table 1. In Table 1, the available numerical (Figs. 4(b) – 4(c)) and experimental values (Fig. 4(a)) for the velocity distribution upstream of a circular intake are compared with results of Eqs. (1) – (6), and the available numerical results for the velocity distribution upstream of a square intake (Fig. 6) are compared with the Eqs. (20) – (24) of the present study. As V_s/V values increases error values also increase due to increase of the effects of boundary friction and shear stresses which are not considered in the potential flow assumption. However, mean percentage error values for all the analysis are below approximately 16% which can be considered acceptable.

The reasons for a larger error between the present study and the study by Bryant et al. (2008, Fig. 3) may be attributed to the followings.

1. They varied the strengths of infinite number of point sinks distributed across the entrance plane of the orifice entrance (depending on the position with the orifice) in their numerical solution.
2. Effect of the step size used in their numerical solution may be present.
3. Size effect (scale effect) of the orifice may be present.
4. Effects of the assumption of ideal fluid flow may be present.

Table 1. Error Analysis of Proposed Equations

	V_s/V	MAE	MSE	RMSE	MPE(%)
Fig. 4(a)	0.2	0.033	0.0015	0.01	4.547
	0.3	0.0259	0.0012	0.01	4.305
Fig. 4(b)	0.2	0.03	0.0011	0.009	4.209
	0.3	0.038	0.0018	0.012	7.151
	0.4	0.0522	0.0033	0.016	12.267
	0.5	0.0576	0.0037	0.017	16.444
Fig. 4(c)	0.02	0.0165	0.0004	0.0053	0.656
	0.05	0.0166	0.0004	0.0057	1.065
	0.1	0.027	0.0012	0.0097	2.537
Fig. 6	0.02	0.0227	0.0007	0.0074	0.809
	0.05	0.0264	0.0011	0.0092	1.518
	0.1	0.0295	0.0014	0.0102	2.461

4. Conclusions

The prediction of the flow field upstream of circular and square intakes is an important subject since it affects sediment or fish entrainment to intakes. In the existing literature, the velocity field was obtained in closed-integral form for the orifices which issued into the atmosphere. In the present study, a practical method has been developed to predict the radial velocity of the flow towards an intake. It has been shown that for both a circular cross-section intake and a square intake, an SSS that has its corresponding imaginary center on the center-line axis downstream of the entrance of the intake can be used for the prediction of the radial velocity within the ambient flow towards the intake. Unlike the previous studies, the proposed method is practical and can predict the radial velocity field for intakes not opening into the atmosphere (submerged outlet), and an intake with a pipe or intake-pipe projecting into the ambient fluid with or without imposed circulation. The agreement between the theoretical results and the available test data and numerical solutions is found to be good. The radial velocity distribution given in the present study may not give satisfactory results in the ambient flow region at and about a rack-type structure sited at the intake-entrance (this may be the main limitation of the present study). SSSs of constant V_s/V indicated in the present study may be used to estimate the flow-dividing streamline(s) or stream surface(s) in the case of more than one intake that requires future studies.

Acknowledgments

The authors would like to thank Gazi University Academic Writing Application and Research Center for proofreading the article.

Nomenclature

A = Intake-entrance cross-section area
a = Side-dimension of a square intake-entrance
A_s = Net effective area of the SSS

A_{sb} = Net effective base area of the SSS
A_{slimit} = Limit magnitude of A_s
D = Internal diameter of a circular intake-entrance
h = Altitude of the spherical sector (cap) of the SSS remaining above the fluid surface
l = Distance between C_o (center of the intake entrance) and C (center of SSS)
l_{limit} = Limit magnitude of l
MAE = Mean average error
MPE = Mean percentage error
MSE = Mean square error
Q = Intake discharge
Q_s = Discharge through the SSS
R = Horizontal distance to the vertical central axis of the intake-entrance
r = Radius of SSS
R_* = Correlation coefficient
RMSE = Root mean square error
r_{limit} = Limit magnitude of r
r_{sb} = Radius of the base of the SSS for the case of SSS ≤ SSS_{limit}
S = Submergence of the center C_o of the intake entrance
SS = Spherical sink
SSS = Spherical sink surface
SSS_{limit} = Limit SSS
SPS = Single point sink
V = Average intake velocity
V_s = Radial velocity at SSS
V_{slimit} = Limit magnitude of V_s
x = Distance of the intersection point B of the SSS and the central-axis line of the intake-entrance to C_o
x_{limit} = Limit magnitude of x
α = Slope angle of the radial line connecting P on SSS and C (center of SSS)
η = Vertical distance of the point P on SSS to the bottom boundary

ORCID

Nevzat Yıldırım https://orcid.org/0000-0002-0985-8084
Kerem Taştan https://orcid.org/0000-0003-1747-2496

References

Acherar L, Jamaleddeen R, Coudour B, Garo JP, Wang HY (2022) Influence of air intake position on heat feedback to the fuel surface in mechanically ventilated compartment - An experimental study. *International Journal of Thermal Sciences* 180:107713, DOI: 10.1016/j.ijthermalsci.2022.107713

Anayiotos AS, Perry GJ, Myers JG, Green DW, Fan PH, Nanda NC (1995) A numerical and experimental investigation of the flow acceleration region proximal to an orifice. *Ultrasound in Medicine and Biology* 21(4):501-516, DOI: 10.1016/0301-5629(94)00141-Y

Bryant DB, Khan AA, Aziz NM (2008) Investigation of flow upstream of orifices. *Journal of Hydraulic Engineering* 134(1):127-133, DOI: 10.1061/(ASCE)0733-9429(2008)134:1(98)

Bytcankova L, Rumann J, Dusicka P (2021) Evaluation of the flow velocity distribution in the intake structure of a small hydropower plant. *IOP Conf. Series: Material Science and Engineering* 1203:022102, DOI: 10.1088/1757-899X/1203/022102

Chanson H, Aoki SI, Maruyama M (2002) Unsteady two-dimensional orifice flow: A large size experimental investigation. *Journal of Hydraulic Research* 40(1):63-71, DOI: 10.1080/00221680209499874

Circiumaru G, Chihaia RA, Voiana A, Nistoran DEG, Simionescu ŞM, El-Leathey LA, Mandrea L (2022) Experimental analysis of a fish guidance system for a river water intake. *Water* 14(3):370, DOI: 10.3390/w14030370

Daggett LL, Keulegan GH (1974) Similitude in free-surface vortex formations. *Journal of Hydraulic Engineering* 100(11):1565-1581, DOI: 10.1061/JYCEAJ.0004105

Giesler MO, Stauch M (1992) Color doppler determination of regurgitant flow: From proximal isovelocity surface areas to proximal velocity profiles. *Echocardiography* 9(1):51-62, DOI: 10.1111/j.1540-8175.1992.tb00439.x

Islam MD, Zhu DZ (2011) Flow upstream of two-dimensional intakes. *Journal of Hydraulic Engineering* 137(1):129-134, DOI: 10.1061/(ASCE)HY.1943-7900.0000284

Kumar VP, Sundaravadivelu R, Murali K (2023) Investigation of proximity effects of offshore intake wells arranged in the vicinity. *Ocean Engineering* 280:114609, DOI: 10.1016/j.oceaneng.2023.114609

Müller M, De Cesare G, Schleiss AJ (2018) Flow field in a reservoir subject to pump-storage operation-in situ measurement and numerical modeling. *Journal of Applied Water Engineering and Research* 6(2):109-124, DOI: 10.1080/23249676.2016.1224692

Naderi V, Farsadizadeh D, Dalir AH, Arvanaghi H (2014) Effect of using vertical plates on vertical intake on discharge coefficient. *Arabian Journal for Science and Engineering* 39(12):8627-8633, DOI: 10.1007/s13369-014-1468-x

Powell DN, Khan AA (2015) Flow field upstream of an orifice under fixed bed and equilibrium scour conditions. *Journal of Hydraulic Engineering* 141(2):04014076, DOI: 10.1061/(ASCE)HY.1943-7900.0000960

Recusani R, Bargiggia GS, Yoganathan AP, Raisaro A, Valdes-Cruz LM, Sung HW, Bertucci C, Gallati M, Moises VA, Simpson IA (1991) A new method for quantification of regurgitant flow rate using color Doppler flow imaging of the flow convergence region proximal to a discrete orifice: An in vitro study. *Circulation* 83(2):594-604, DOI: 10.1161/01.cir.83.2.594

Roshan R, Ghobadian R (2023) The effect of reservoir geometry on the critical submergence depth in hydroelectric power plants intake. *Applied Water Science* 13(7):155, DOI: 10.1007/s13201-023-01960-z

Sarkardeh H, Jabbari E, Zarrati AR, Tavakkol S (2014) Velocity field in a reservoir in the presence of an air-core vortex. *Proceedings of the Institution of Civil Engineers-Water Management* 167(6):356-364, DOI: 10.1680/wama.13.00046

Shammaa Y, Zhu DZ, Rajaratnam N (2005) Flow upstream of orifices and sluice gates. *Journal of Hydraulic Engineering* 131(2):127-133, DOI: 10.1061/(ASCE)0733-9429(2005)131:2(127)

Sinha S (2022) Power intake size optimization for economical hydropower. *Results in Engineering* 15:100572, DOI: 10.1016/j.rineng.2022.100572

Taştan K (2016) Critical submergence for isolated and dual rectangular intakes. *Sadhana-Academy Proceedings in Engineering Sciences* 41(4):425-433, DOI: 10.1007/s12046-016-0474-y

Taştan K, Yıldırım N (2018) Effects of intake geometry on the occurrence of a free-surface vortex. *Journal of Hydraulic Engineering* 144(4):

04018009, DOI: 10.1061/(ASCE)HY.1943-7900.0001439
Taştan K, Erat B, Barbaros E, Eroğlu N (2023) Flow boundary effects on scour characteristics upstream of pipe intakes. *Ocean Engineering* 278:114343, DOI: 10.1016/j.oceaneng.2023.114343
Xu H, Cao Z, Wang Q (2023a) Experimental investigation on reservoir sediment flushing through a bottom tunnel with an initially covered intake. *Journal of Hydraulic Engineering* 149(8):04023024, DOI: 10.1061/JHEND8.HYENG-13580
Xu C, Tian J, Liu Z, Wang R, Wang G (2023b) Three-dimensional reverse modeling and hydraulic analysis of the intake structure of pumping stations on sediment-laden rivers. *Water Resources Management* 37(1):537-555, DOI: 10.1007/s11269-022-03385-w
Yıldırım N (2004) Critical submergence for a rectangular intake. *Journal of Engineering Mechanics* 130(10):1195-1210, DOI: 10.1061/(ASCE)0733-9399(2004)130:10(1195)
Yıldırım N, Kocabaş F (1995) Critical submergence for intakes in open channel flow. *Journal of Hydraulic Engineering* 121(12):900-905, DOI: 10.1061/(ASCE)0733-9429(1995)121:12(900)
Yıldırım N, Kocabaş F, Gülcan SC (2000) Flow-boundary effects on critical submergence of intake pipe. *Journal of Hydraulic Engineering* 126(4):288-297, DOI: 10.1061/(ASCE)0733-9429(2000)126:4(288)
Yıldırım N, Kocabaş F, Gülcan SC (2007) Errata for "Flow-boundary effects on critical submergence of intake pipe". *Journal of Hydraulic Engineering* 133(4):461, DOI: 10.1061/(ASCE)0733-9429(2007)133:4(461)

Appendix I

An Example for the Trial-and-Error Solution

As an example, let us find the geometrical location (SSS) of the points that have $V_s/V = 0.10$ in the study by Shammaa et al. (2005, Fig. 4, square orifice intake entrance was flush with the vertical rear-wall, distances of the side walls and the bottom floor boundary were sufficiently large, note that they gave the isovel contours for the upper half of the square intake). From Eqs. (2); (3) and (19), get $l/a = 0.4(0.1)^{0.624} = 0.095$, and $A/A_s = a^2/A_s = V_s/V = 0.10$; compute $A_s = 10A$ or, $A_s/a^2 = 10$. Since $l/a = 0.095$ is known, the center C of the SSS is located and denoted by $C_{0.1}$ in Fig. 6. The distance of the vertical rear-wall to the center $C_{0.1}$ of the SSS is equal to l that is less than r. Therefore, the vertical rear-wall intersects the SSS and it has a blockage effect on SSS. The distances of the left and right-side walls, and the bottom floor-boundary to the center C of the SSS are sufficiently large {larger than or equal to the magnitudes of r or thereby $(r^2 - l^2)^{1/2}$ or $[(r/a)^2 - (l/a)^2]^{1/2}$ relating to their solution} due to which these boundaries do not intersect the SSS. Thus, the left and right-side walls, and the bottom floor-boundary have no blockage effects on SSS. Note that for the computation of boundary blockages of the sidewalls, bottom boundary, rear-wall (if there exists) and the intake pipe itself for an intake (or SSS) in a rectangular prism one can refer to the studies by Yıldırım et al. (2000, 2007) and Yıldırım (2004).

First Trial

Let choose $r/a = 2$ for which SSS is not drawn in Fig. 6 (since it is not the final trial solution not to make the figure crowded the SSS is not drawn, if wanted it can be drawn). Check that $r/a = 2$ is smaller than the distances (clearances) of the side walls and the bottom floor boundary to the center $C_{0.1}$ of the SSS thereby also $[(r/a)^2 - (l/a)^2]^{1/2} = [(2)^2 - (0.095)^2]^{1/2} = 1.997$ is smaller than the distances of the side walls and the bottom floor boundary to the center $C_{0.1}$ of the SSS (in conjunction with assumptions in the study by Shammaa et al., 2005, Fig. 4, square orifice intake entrance)]. Therefore, the side walls and the bottom floor boundary have no

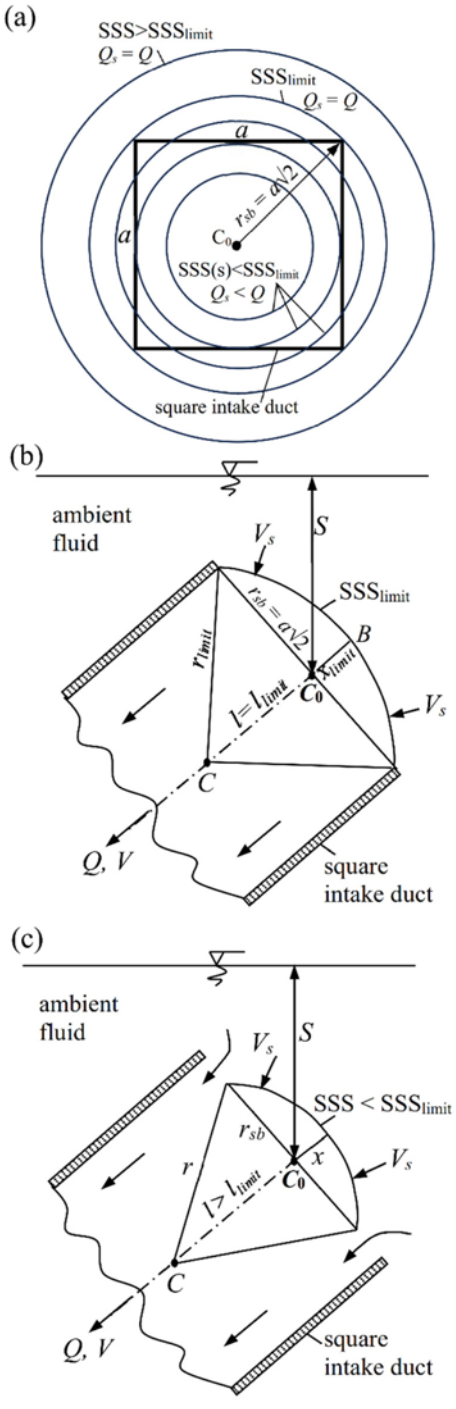


Fig. 7. SSS and SSS_{limit} : (a) Square Intake Duct, (b) SSS = SSS_{limit}, (c) SSS < SSS_{limit} for a Square Intake

blockage effects on SSS. Only the vertical rear-wall has a blockage effect on SSS as stated earlier.

In this example, it is geometrically simple to compute A_s that is $A_s = 2\pi rx = 2\pi r(r - l)$ or, $(A_s/a^2) = 10 = 2\pi(r/a)(r/a - l/a) = 2\pi(r/a)(r/a - 0.095)$ that yields $r/a = 1.31$ (computed). Since both magnitudes of the chosen r/a (= 2) and computed r/a (= 1.31) are not equal, the solution is not correct. Therefore, choose a new magnitude for r/a and repeat the solution.

Second Trial

To prevent this paper being excessively long, only the solution of the final trial is given herein. Let choose $r/a = 1.31$ for which SSS is drawn in Fig. 6. Since $r/a = 1.31$ is smaller than the distances of the side walls and the bottom floor boundary to the center $C_{0.1}$ of the SSS thereby also $[(r/a)^2 - (l/a)^2]^{1/2} = [(1.31)^2 - (0.095)^2]^{1/2} = 1.306$ is smaller than the distances of the side walls and the bottom floor boundary to the center $C_{0.1}$ of the SSS (in conjunction with assumptions in the study by Shammaa et al., 2005, Fig. 4 square orifice intake entrance)] the side walls and the bottom floor boundary have no blockage effects on SSS. Only the vertical rear-wall has a blockage effect on SSS as stated earlier.

$A_s = 2\pi rx = 2\pi r(r - l)$ or, $(A_s/a^2) = 10 = 2\pi(r/a)(r/a - l/a) = 2\pi(r/a)(r/a - 0.095)$ that yields $r/a = 1.31$ (computed). Since both magnitudes of the chosen r/a (= 1.31) and computed r/a (= 1.31) are equal, the solution is correct (no need to choose a new magnitude for r/a and repeat the solution). $x/a = (r/a - l/a) = (1.31 - 0.095) = 1.215$.